

The jet-disk symbiosis without *maximal jets*: 1-D hydrodynamical jets revisited

Patrick Crumley¹, Chiara Ceccobello¹, Riley M. T. Connors¹, Yuri Cavecchi^{1,2,3}

¹Anton Pannekoek Institute for Astronomy, University of Amsterdam, P.O. Box 94249, 1090 GE Amsterdam, the Netherlands

²Department of Astrophysical Sciences, Princeton University, Peyton Hall, Princeton, NJ 08544, USA

³Mathematical Sciences and STAG Research Centre, University of Southampton, SO17 1BJ, UK

e-mail: p.k.crumley@uva.nl

September 12, 2018

ABSTRACT

In this work we discuss the recent criticism by Zdziarski (2016) of the *maximal jet* model derived in Falcke & Biermann (1995). We agree with Zdziarski that in general a jet’s internal energy is not bounded by its rest-mass energy density. We describe the effects of the mistake on conclusions that have been made using the *maximal jet* model and show when a *maximal jet* is an appropriate assumption. The *maximal jet* model was used to derive a 1-D hydrodynamical model of jets in `agnjet`, a model that does multiwavelength fitting of quiescent/hard state X-ray binaries and low-luminosity active galactic nuclei. We correct algebraic mistakes made in the derivation of the 1-D Euler equation and relax the *maximal jet* assumption. We show that the corrections cause minor differences as long as the jet has a small opening angle and a small terminal Lorentz factor. We find that the major conclusion from the *maximal jet* model, the jet-disk symbiosis, can be generally applied to astrophysical jets. We also show that isothermal jets are required to match the flat radio spectra seen in low-luminosity X-ray binaries and active galactic nuclei, in agreement with other works.

1. Introduction

In this work we reexamine the *maximal jet* model of accreting black-holes with disks and jets derived in Falcke & Biermann (1995). The idea behind a *maximal jet* is that there is a strict upper limit on the power carried by a jet in terms of its mass flux. As first pointed out by Zdziarski (2016), the *maximal jet* is the result of an erroneous conclusion that the internal energy density of a gas must be less than or equal to the rest-mass energy density of the gas. The *maximal jet* model was used to link the power carried by the jet to the power in the accretion disk, arriving at the highly influential and widely used “jet-disk symbiosis.” The main result of the jet-disk symbiosis states that the total power in the jet, L_j , can be related to the mass accretion rate of the disk, \dot{M}_{disk} , through the jet’s Lorentz factor γ_j and an efficiency, $\eta < 1$. $L_j = \eta\gamma_j\dot{M}_{\text{disk}}c^2$.

Without appealing to a *maximal jet*, we argue in this paper that the jet-disk symbiosis is reasonable for astrophysical accreting black-holes in general. In fact, it is reasonable to estimate the power of the jet to be $\lesssim \eta\dot{M}_{\text{disk}}c^2$, as long as one takes $\eta \lesssim$ a few, as opposed to being strictly less than one. It is intuitive why this conclusion should hold in a Blandford-Payne type jet where the disk itself is powering the jet (Blandford & Payne 1982), but the conclusion should also hold for jets that are powered by the black hole’s rotational energy via the Blandford-Znajek mechanism (Blandford & Znajek 1977). In the Blandford-Znajek mechanism, the jet power is proportional to the poloidal magnetic flux at the black hole, and the magnetic flux that can be carried to the black hole is ultimately limited by the mass-accretion rate (Narayan et al. 2003; Tchekhovskoy et al. 2011). This explains why the jet-disk symbiosis has been such a successful concept.

However, the *maximal jet* conclusion results solely from an algebraic mistake in Falcke & Biermann (1995) and cannot be

applied broadly to accreting black-holes with jets. We argue in this work that if the jet is efficiently accelerated and has a small terminal Lorentz factor, the initial enthalpy should be roughly equal to the rest-mass energy, in agreement with a *maximal jet*. A jet with a large terminal Lorentz factor will start with a large enthalpy, but if the jet is efficiently accelerated, the internal energy of the jet will be approximately equal to the rest-mass energy density after the jet has reached its final Lorentz factor (Vlahakis & Königl 2003; McKinney 2006). There are some cases when this approximation breaks down. For a steady-state, axisymmetric, magnetically-accelerated outflow to be efficiently accelerated, it must stay causally connected in the transverse direction. However, it is unclear if this requirement is an actual impediment to the magnetic acceleration of astrophysical jets, or an artifact of the symmetries imposed. (For a concise review of magnetic acceleration of jets, see Komissarov 2011.) A radiation or thermal pressure-driven jet will be efficiently accelerated even if it is conical and free-streaming. We assume the jet opening angle is small enough to ensure it remains in causal contact with the external medium throughout this paper.

In addition, we correct algebraic errors made in the derivation of the jet’s Lorentz factor as a function of distance in Falcke (1996). This Lorentz factor profile is used to calculate the dynamics of a jet in `agnjet`, an outflow dominated model of low-luminosity accreting black holes that has been applied to several different low-luminosity active galactic nuclei and X-ray binaries (Markoff et al. 2005, 2008; Maitra et al. 2009; van Oers et al. 2010; Markoff et al. 2015; Plotkin et al. 2015; Connors et al. 2017). The physics behind `agnjet` is presented in detail in Markoff et al. (2005) & Maitra et al. (2009). We characterize how the changes to the Lorentz factor profile effect the resulting spectral energy distribution calculated by `agnjet`. We find that the aforementioned algebraic mistakes have a negligible effect on the radiation from the outflow as long as the jet is roughly

isothermal, has a small Lorentz factor, and is launched with an aspect ratio of order unity.

Our paper is organized as follows: in Section 2 we outline the mistake made when the *maximal jet* was derived. Then, we argue why the main conclusion of the *maximal jet* model, the jet-disk symbiosis, still holds. We also describe the systems for which the *maximal jet* model can be applied. In Section 3, we re-examine 1-D pressure-driven jets, relaxing the *maximal jet* requirement. In Section 4, we make the dynamics of `agnjet` self-consistent, and find the combined effects of all the changes to the dynamics on the calculated spectral energy distribution are small. We end by summarizing and discussing our results.

2. Bernoulli's equation and Maximal Jets

The total power of an axisymmetric, conical jet at height z from the launching point with an opening angle θ is equal to the jet's Lorentz factor γ_j times the enthalpy flux,

$$L_j = \gamma_j^2 \beta_j c \omega \pi z^2 \sin^2 \theta, \quad (1)$$

where ω is the enthalpy. In ideal magneto-hydrodynamics (MHD), a baryonic jet with a co-moving number density of protons n , has an enthalpy given by

$$\omega = nm_p c^2 + U_j + P_j = nm_p c^2 + U_{\text{th}} + P_{\text{th}} + \frac{B^2}{4\pi}. \quad (2)$$

U_j, P_j are the total energy density and pressure of the jet, which can be broken down into a gas component ($U_{\text{th}}, P_{\text{th}}$) and a magnetic component ($U_B = P_B = B^2/8\pi$).¹ The jet's gas pressure can be related to the internal energy of the gas via the adiabatic index, Γ , $P_{\text{th}} = (\Gamma - 1)U_{\text{th}}$. We define the magnetization parameter, σ , as $B^2/(4\pi nm_p c^2)$.² The enthalpy then simplifies to

$$\omega = nm_p c^2 \left[1 + \sigma + \frac{\Gamma U_{\text{th}}}{nm_p c^2} \right] \quad (3)$$

In Falcke & Biermann (1995), the authors assume that the magnetic fields are isotropically turbulent, and therefore can be treated as an ideal gas with adiabatic index Γ . The authors then write the enthalpy in terms of the total jet internal energy density U_j as

$$\omega \sim nm_p c^2 + \Gamma U_j \quad (4)$$

The authors then re-write the enthalpy in terms of the sound speed, β_s , adiabatic index, and density. The sound speed is

$$\beta_s^2 = \frac{\Gamma P_j}{\omega} = \frac{\Gamma(\Gamma - 1)U_j}{\omega}, \quad (5)$$

(see e.g. Königl 1980). From Equations (4) & (5), one can derive the well known result that the maximal sound speed is $\sqrt{\Gamma - 1}$. Substituting Equation (5) into Equation (4) and solving for ω yields

$$\omega = \frac{nm_p c^2}{1 - \beta_s^2/(\Gamma - 1)} \quad (6)$$

¹ The gravitational potential energy and the radiation pressure and energy density contributions to the enthalpy are neglected in this work.

² Our σ is the same as the more standard magnetization parameter σ in the “force-free” MHD regime. We neglect the gas pressure contributions to σ to simplify the equations.

Compare the above equation to the equivalent equation in Falcke & Biermann (1995). They give a formula that is the approximation when β_s is small,

$$\omega \approx nm_p c^2 \left(1 + \frac{\beta_s^2}{\Gamma - 1} \right) \quad \text{when } \beta_s \ll \sqrt{\Gamma - 1}. \quad (7)$$

The mistake is that Falcke & Biermann (1995) then use Equation (7) to argue ω must be less than $2nm_p c^2$ because β_s must be less than $\sqrt{\Gamma - 1}$. Clearly this is wrong, because when using the correct formula, Equation (6), ω diverges to infinity as $\beta_s \rightarrow \sqrt{\Gamma - 1}$. This mistake was first pointed out by Zdziarski (2016).

Since the total jet power is equal to the Lorentz factor times the enthalpy flux, the mistake leads to a maximal jet power $L_j \leq 2\gamma_j \dot{M}_j c^2$, where \dot{M}_j is the mass flux through the jet. Protons are not created at the jet base, so Falcke & Biermann (1995) argue $\dot{M}_j \leq \dot{M}_{\text{disk}}$, where \dot{M}_{disk} is the mass accretion rate of the disk. Therefore, Falcke & Biermann (1995) conclude $L_j \sim \eta \gamma_j \dot{M}_{\text{disk}} c^2$, $\eta \leq 1$, i.e., the jet-disk symbiosis. The mass flux through the jet could be larger than \dot{M}_{disk} if the jet has significant baryon loading from winds. If the disk drives a strong wind, the disk wind may be able to increase the baryon loading, but it is generally thought that in X-ray binaries a strong disk wind is associated with the soft states, i.e., when the jet is not present (Nielsen & Lee 2009). New evidence shows simultaneous winds and jets in the high state, but there is no evidence that shows a strong wind during the low hard-state (Muñoz-Darias et al. 2016; Kalemci et al. 2016; Muñoz-Darias et al. 2017). Stellar winds could also play a role in increasing \dot{M}_j in AGN or high-mass X-ray binaries (Komisarov 1994). At any rate, the baryon loading would only significantly increase the power carried by the jet when the power of the intercepted baryons exceeds that of the jet.

It is a reasonable approximation that the power of the jet does not significantly exceed $\dot{M}_{BH} c^2$ even if the power in the jet is supplied by the spin of the black hole via the Blandford-Znajek mechanism. In the Blandford-Znajek mechanism, the power extracted is proportional to the magnetic flux carried to the black hole (Blandford & Znajek 1977). The magnetic flux carried to the black-hole is proportional to \dot{M}_{BH} , and GRMHD simulations find that the resultant jet power exceeds $\dot{M}_{BH} c^2$ by a factor of at most ~ 3 (Tchekhovskoy et al. 2011). However, there is no general requirement that the resultant jet's power is dominated by the jet's kinetic energy throughout the jet. For instance, in a Poynting-dominated jet, the power is $L_j = \gamma_j \dot{M}_j c^2 (1 + \sigma)$ and σ can be $\gg 1$. Clearly, the enthalpy flux can be much larger than the mass flux, but in the next subsection, we will argue from completely different grounds than Falcke & Biermann (1995) that while a jet can start with any initial enthalpy, the jet will reach an $\omega/nm_p c^2 \sim 2$ at the modified magneto-sonic fast point if it is efficiently accelerated. Furthermore, in efficiently accelerated jets that have mildly relativistic terminal Lorentz factors, i.e., $\gamma_j \beta_j \sim 1$, the initial enthalpy will not exceed the rest mass energy density by a significant amount. The reason why this is true can be seen most easily via Bernoulli's equation.

2.1. Bernoulli's equation

In a steady-state, conservative jet, the total power carried by the jet is constant along the jet. Dividing the power by another conserved quantity, the particle number flux through a cross-section of the jet, one re-derives the relativistic Bernoulli's equation (see

e.g. Königl 1980):

$$\gamma_j \frac{\omega}{n} = \text{constant}. \quad (8)$$

Bernoulli's equation is simply a statement that the energy of the fluid per particle must not change as the particles travel along a streamline, as long as particles are not created or destroyed. In this paper we are only considering self-similar jets with no gradient of the pressure in the toroidal direction of the jet. If a jet is launched with an initial Lorentz factor γ_0 with an initial enthalpy per particle of ω_0/n_0 , then because $\omega/n \geq m_p c^2$, it is clear from Eq (8) and (3) there is a maximal Lorentz factor:

$$\gamma_{\max} = \gamma_0 \frac{\omega_0}{n_0 m_p c^2} = \gamma_0 \left[1 + \sigma_0 + \frac{\Gamma U_{\text{th},0}}{n_0 m_p c^2} \right]. \quad (9)$$

If a jet achieves γ_{\max} , it means it has converted 100% of its Poynting and thermal energy into bulk kinetic energy. Doing so in a steady-state, Poynting-dominated jet requires that the jet be causally connected in the transverse direction.³ If the jet goes out of causal contact in the transverse direction, the magnetic pressure may not be able to accelerate the jet further. If the flow is completely spherical with $\sigma_0 \gg 1$, the outflow reaches a terminal Lorentz factor $\sim \sigma_0^{1/3}$ (Goldreich & Julian 1970). If instead the jet has an opening angle θ_j , the terminal Lorentz factor is $\gamma_f = \min(\sigma_0, \sigma_0^{1/3} \theta_j^{-2/3})$ (Kumar & Zhang 2015). When the jet is thermally or radiatively driven, equation (9) should hold regardless of the jet's geometry. Vlahakis & Königl (2003); Komissarov et al. (2007) show that in some Poynting dominated jets, electromagnetic fields will naturally self-collimate the jet and ensure that the jet remains causally connected up to the modified magneto-sonic fast point. In doing so the jet reaches rough equipartition between kinetic flux and Poynting flux, and the jet reaches a final Lorentz factor equal to $\sim \frac{1}{2} \omega_0 / n_0 m_p c^2$.⁴ Therefore, using Bernoulli's equation, the jet should have $\omega/n m_p c^2 \sim 2$ at the modified magneto-sonic fast point, right after the jet has finished accelerating. Furthermore, $\omega_0/n_0 m_p c^2 \approx 2$ is likely to be a good assumption for mildly-relativistic outflows with $\gamma_j \beta_j$ of order unity, because if $\omega_0 \gg n_0 m_p c^2$ the jets would reach γ_j that are too large. Mildly relativistic jets are expected to occur in quiescent/hard state black-hole x-ray binaries⁵ (Gallo et al. 2003; Miller-Jones et al. 2007). A mildly relativistic jet may be launched by the super-massive black-hole at the center of our galaxy, Sgr A* (Falcke et al. 2009; Brinkerink et al. 2015).

Therefore, $\omega_0/n_0 \sim 2 m_p c^2$ should be a fine assumption as long as we restrict ourselves to mildly relativistic outflows with small enough opening angles. In jets with large Lorentz factors, $\gamma_j \beta_j \gg 5$, like blazars, BL Lacs, relativistic tidal disruption events, and gamma-ray bursts, $\omega_0/n_0 \gg 2 m_p c^2$, but if the jet is accelerated efficiently, at the modified magneto-sonic fast point $\omega/n m_p c^2 \sim 2$.⁶ The previous jet model of `agnjet`, and the one described in this paper, are not capable of reproducing the jets in these objects.

³ The requirement that Poynting-dominated jets remain causally connected in the transverse direction can be relaxed if the outflow is impulsive (Granot et al. 2011)

⁴ The jet is launched with a sub-relativistic velocity, $\gamma_0 = 1$

⁵ Although see Heinz & Merloni (2004); Miller-Jones et al. (2006) regarding the difficulties in placing a strong upper limit on the Lorentz factor of X-ray binaries.

⁶ If the highly relativistic jet is comprised of electron-positron pairs, then $\omega_0/n_0 \gg 2 m_e c^2$.

In the process of examining the *maximal jet* model, we have discovered additional minor algebraic mistakes in the Lorentz factor profile derived in Falcke (1996) and used in `agnjet`. In the rest of the paper, we show that these mistakes are minor and do not affect the conclusions drawn from fitting the model to low Lorentz factor sources. We then show that isothermal or nearly isothermal jets are required to have a flat radio spectrum.

3. Pressure-Driven Conical Jets

In this section we reproduce with minor corrections the derivation of the one-dimensional propagation of a quasi-isothermal hydrodynamic jet from Falcke (1996). We find that the corrected quasi-isothermal acceleration profile agrees within $\sim 20\%$ with the result in Falcke (1996), and the corrected Lorentz factor profile is much closer to the profile in a perfectly isothermal flow (see Figure 1).

The one-dimensional propagation of a supersonic jet in the z direction follows the Euler equation given in Pomraning (1973); Falcke et al. (2009):

$$\gamma_j \beta_j n \frac{\partial}{\partial z} \left\{ \gamma_j \beta_j \frac{\omega}{n} \right\} = - \frac{\partial P_j}{\partial z} \quad (10)$$

Following Falcke & Biermann (1995), we assume that the jet is well-described by a fluid with adiabatic index $4/3$ and use the enthalpy from Eq (4)

$$\omega = n m_p c^2 + \Gamma U_j, \quad (11)$$

so Eq (10) becomes:

$$\gamma_j \beta_j n \frac{\partial}{\partial z} \left\{ \gamma_j \beta_j \left(m_p c^2 + \frac{\Gamma U_j}{n} \right) \right\} = -(\Gamma - 1) \frac{\partial U_j}{\partial z}. \quad (12)$$

Particle number conservation along the jet forces the number density to be

$$n_j = n_0 \left(\frac{\gamma_j \beta_j}{\gamma_0 \beta_0} \right)^{-1} \left(\frac{z}{z_0} \right)^{-2} \left(\frac{\sin \theta}{\sin \theta_0} \right)^{-2}, \quad (13)$$

where θ is the opening angle of the jet (i.e. the cross-sectional radius of the jet divided by the height of the jet).

The jet is launched at an initial height of z_0 , and is assumed to be traveling at the sound speed. The sound speed in the jet's rest frame, β_s , is

$$\beta_s^2 = \frac{\Gamma P_j}{\omega} = \frac{\Gamma(\Gamma - 1) U_j}{n m_p c^2 + \Gamma U_j}. \quad (14)$$

Instead of requiring $U_j = n m_p c^2$ throughout the jet, we introduce a new parameter ζ , which is the ratio between the initial internal energy of the jet and the initial rest-mass energy density, i.e., $U_0 = \zeta n_0 m_p c^2$. $\zeta = 1$ corresponds to the maximal jet conditions in Falcke (1996). The initial sound speed at the base of the jet is

$$\beta_{s0} = \sqrt{\frac{\zeta \Gamma (\Gamma - 1)}{1 + \zeta \Gamma}}. \quad (15)$$

For $\zeta = 1$, $\Gamma = 4/3$ the sound speed is ≈ 0.43 . Since the jet is assumed to be launched traveling at the sound speed, the initial velocity of the jet is

$$\gamma_0 \beta_0 = 1 / \sqrt{\beta_{s0}^{-2} - 1} = \sqrt{\frac{\zeta \Gamma (\Gamma - 1)}{1 + 2\zeta \Gamma - \zeta \Gamma^2}}. \quad (16)$$

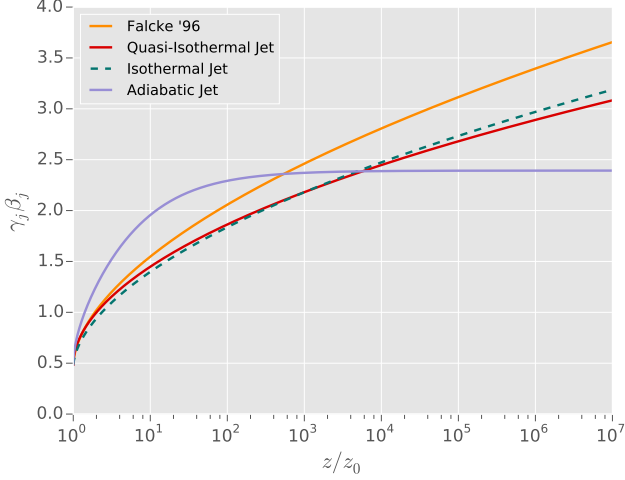


Fig. 1. This figure shows the difference between the Lorentz factor profile derived in Falcke (1996) and used in `agnjet` c.f. Markoff et al. (2005) (yellow solid line), the derived Lorentz factor profile after correcting for algebraic mistakes (eq 18, red solid line), the 1-D Euler equation in a conical jet assuming continual heating of the jet by an outside source such that the jet is isothermal, $U_j = nm_p c^2$ (green dashed line), and the Euler equation in an adiabatic jet, where $U_j = n_0 m_p c^2 (n/n_0)^\Gamma$ (lilac solid line). If the jet follows Bernoulli's equation, $\gamma_{\max} \beta_{\max} \approx 2.39$ when $\gamma_0 \beta_0 \approx 0.485$ and $\Gamma = 4/3$ —precisely the terminal value in the adiabatic jet Lorentz factor profile.

For $\Gamma = 4/3$, $\zeta = 1$, $\gamma_0 \beta_0 \approx 0.485$.

The jet Lorentz factor profile from Falcke (1996) can be derived by treating the jet as a conical jet ($\theta = \theta_0$) and using particle number conservation to get a z dependence on the density (see Eq 13). To fix the z dependence on the internal energy, we need a prescription of how the temperature changes with a change in density. If the jet is isothermal, T_j is constant and $U_e \propto n$. If the jet is adiabatic, $U_e \sim nkT_j \propto n^\Gamma$, and therefore $T_j \propto n^{\Gamma-1} \propto (\gamma_j \beta_j)^{1-\Gamma} z^{2-2\Gamma}$. Falcke (1996) assumes that the gas is only able to do PdV work in the z -direction, hence the only adiabatic losses are due to the jet's acceleration. We call this assumption quasi-isothermal. If the jet is quasi-isothermal, the temperature T_j is proportional to $(\gamma_j \beta_j)^{1-\Gamma}$. It is difficult to understand how exactly the gas is prevented from doing PdV work in the lateral direction. It is far more realistic to assume there is continuous particle acceleration to counteract the adiabatic losses due to the expansion, as Blandford & Königl (1979) use to explain their isothermal jet model. For a heating mechanism to recover the quasi-isothermal temperature dependence, it means it must be capable of compensating the large adiabatic losses due to the lateral expansion, but not the comparatively small adiabatic losses from the acceleration. Why the heating mechanism would do this is unclear. We retain $T_j \propto (\gamma_j \beta_j)^{1-\Gamma}$ here for historical reasons, and we note that when using the correct Euler equation, the difference between the quasi-isothermal case and the isothermal case is negligible for the small Lorentz factors achieved in jets with $U_{j,0} \sim n_0 m_p c^2$ and $\Gamma = 4/3$, as assumed in this work.

In a quasi-isothermal jet, U_j is

$$U_j = \zeta n_0 m_p c^2 \left(\frac{\gamma_j \beta_j}{\gamma_0 \beta_0} \right)^{-\Gamma} \left(\frac{z}{z_0} \right)^{-2}. \quad (17)$$

Substituting Eqs (17) and (13) into Eq (10), and assuming the jet is launched with an initial $\gamma_0 \beta_0$ equal to the sound speed

(Eq 16), the 1-D Euler equation that results is

$$\left\{ \gamma_j \beta_j \frac{\Gamma + \xi}{\Gamma - 1} - \Gamma \gamma_j \beta_j - \frac{\Gamma}{\gamma_j \beta_j} \right\} \frac{\partial \gamma_j \beta_j}{\partial z} = \frac{2}{z}; \quad (18)$$

$$\xi = \frac{1}{\zeta} \left(\frac{\gamma_j \beta_j}{\gamma_0 \beta_0} \right)^{\Gamma-1}; \quad \gamma_0 \beta_0 = \sqrt{\frac{\zeta \Gamma (\Gamma - 1)}{1 + 2\zeta \Gamma - \zeta \Gamma^2}}. \quad (19)$$

The above equation should reduce to the jet Lorentz factor profile used in Falcke (1996); Markoff et al. (2005) when $\zeta = 1$. However, it differs from Eq (2) in Falcke (1996):

$$\left\{ \gamma_j \beta_j \frac{\Gamma + \xi}{\Gamma - 1} - \frac{\Gamma}{\gamma_j \beta_j} \right\} \frac{\partial \gamma_j \beta_j}{\partial z} = \frac{2}{z}; \quad (20)$$

$$\xi = \left(\gamma_j \beta_j \frac{\Gamma + 1}{\Gamma (\Gamma - 1)} \right)^{1-\Gamma} \quad (21)$$

The difference between our equation and the equation in Falcke (1996) can be accounted for as follows: the $-\Gamma \gamma_j \beta_j$ term in Eq (18) results from a neglected $\frac{\partial}{\partial z} (U_j/n)$ term, the difference in the exponent in ξ results from an arithmetic error, and finally the difference in the inside of the parenthesis of ξ terms is from setting $\gamma_0 \beta_0 = \beta_{s0}^2$ instead of using the proper value given in Eq (16). The difference between the solutions of Eqs (18) and (20) are small and shown in Figure 1. In Figure 1, we also include solutions to the 1-D Euler equations when the jet is isothermal ($T_j = \text{constant}$, i.e., Eq 20 with $\xi = 1$) and adiabatic ($T_j \propto (\gamma_j \beta_j)^{1-\Gamma} z^{2-2\Gamma}$, see Eq 25).

The above quasi-isothermal and isothermal solutions do not conserve energy, nor do they follow the Bernoulli equation. The violation of Bernoulli's equation is clear by looking at maximal Lorentz factor on any pressure driven jet that conserves energy, with $U_0 = \zeta n_0 m_p c^2$, Eq (9) becomes

$$\gamma_{\max} = \gamma_0 (1 + \Gamma \zeta), \quad (22)$$

or $\gamma_{\max} = 7\gamma_0/3$ for a relativistic gas starting with equal parts internal energy density and rest mass energy density, $U_0 = n_0 m_p c^2$. All solutions except for the adiabatic solution eventually reach a γ_j that exceeds γ_{\max} , which is easily seen in Figure 1.

The total amount of heating needed to explain the solution in `agnjet` is equivalent to the increase in the jet power. Using Eq (1) for the jet's total power, the increase of power in a quasi-isothermal jet is

$$\frac{L_j}{L_0} = \frac{1}{1 + \Gamma} \frac{\gamma_j}{\gamma_0} \left[1 + \Gamma \left(\frac{\gamma_j \beta_j}{\gamma_0 \beta_0} \right)^{1-\Gamma} \right]. \quad (23)$$

The required heating to power a quasi-isothermal jet is shown in Figure 2. The heating must come from some internal process in the jet, but the heating mechanism is not capable of being captured by our time-independent, laminar flow treatment in this work. One possibility is that heating originates from internal shocks (Malzac 2013). Internal shocks would do more than just heat the gas, they would also change the momentum and hence the dynamics. Magnetic reconnection can convert magnetic energy into thermal energy to keep the jet's electrons isothermal, but reconnection would not increase the total power carried by the jet.

The jet will conserve energy if instead of assuming $T_j \propto (\gamma_j \beta_j)^{1-\Gamma}$, we use an adiabatic jet where $U_j \propto n^\Gamma$, or $T_j \propto$

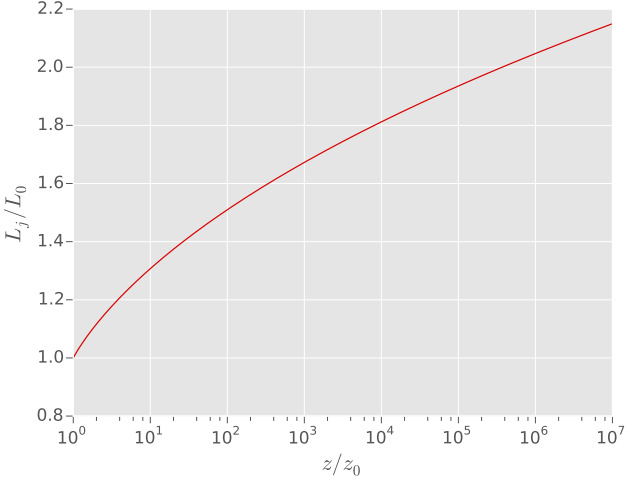


Fig. 2. This plot shows the total power carried by a quasi-isothermal jet as a function of distance from the black hole z normalized to its initial power. The power of the jet increases as it propagates (see Equation 23). One possibility to explain how the jet is heated is via some internal process not captured by the time-independent Euler equation, such as internal shocks.

$(\gamma_j \beta_j)^{1-\Gamma} z^{2-2\Gamma}$. In an adiabatic conical jet the z dependence of the internal energy is:

$$U_j = \zeta n_0 m_p c^2 \left(\frac{\gamma_j \beta_j}{\gamma_0 \beta_0} \right)^{-\Gamma} \left(\frac{z}{z_0} \right)^{-2\Gamma}, \quad (24)$$

and the full 1-D Euler equation is

$$\left\{ \gamma_j \beta_j \frac{\Gamma + \xi}{\Gamma - 1} - \Gamma \gamma_j \beta_j - \frac{\Gamma}{\gamma_j \beta_j} \right\} \frac{\partial \gamma_j \beta_j}{\partial z} = \frac{2\Gamma}{z} (1 + \gamma_j^2 \beta_j^2); \quad (25)$$

$$\xi = \frac{1}{\zeta} \left(\gamma_j \beta_j \sqrt{\frac{1 + 2\zeta\Gamma - \zeta\Gamma^2}{\zeta\Gamma(\Gamma - 1)}} \right)^{\Gamma-1} \left(\frac{z}{z_0} \right)^{2(\Gamma-1)}. \quad (26)$$

The solution to the adiabatic 1-D Euler equation when $\zeta = 1$ is shown in Figure 1. Unlike the quasi-isothermal case, the jet reaches the maximal Lorentz factor equal to that predicted by the Bernoulli equation $\gamma_0(1 + \Gamma)$.

4. Radiation, Collimation, and a more Self-Consistent *agnjet*

The *agnjet* model was developed in Markoff et al. (2005); Maitra et al. (2009) as way of fitting multi-wavelength spectra of black-hole jets. The model is described in full detail in the aforementioned papers, but we will give a brief description here. In *agnjet* the gas is assumed to be moving at a velocity equal to the sound speed through a nozzle with constant radius r_0 that ends at z_0 . At z_0 , the jet is allowed to expand at constant velocity equal to the sound speed⁷ in the cross-section radial direction, and weakly accelerated in the z direction by the jet's pressure, i.e., it follows the 1-D Euler equation in the z direction. Electrons initially have a Maxwell-Jüttner thermal distribution in the nozzle and the jet, and a fraction of the electrons are accelerated into a non-thermal population at a height z_{acc} . The electrons radiate via synchrotron and inverse Compton processes.

⁷ $\gamma_s \beta_s = \gamma_0 \beta_0$

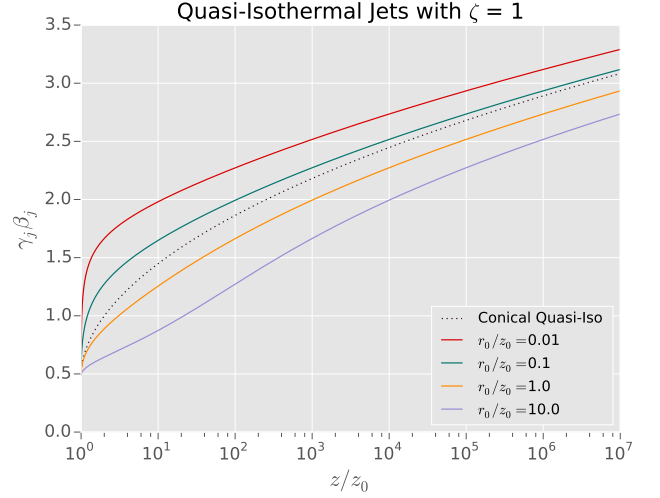


Fig. 3. This figure shows how a different initial aspect ratio of the jet, r_0/z_0 , changes the dynamics of a self-collimated quasi-isothermal jet compared to the conical jet considered in Figure 1. As long as $r_0/z_0 \sim 1$, the difference between a conical and self-collimated jet is much less than a factor of 2.

The assumption of a lateral expansion at constant speed while accelerating vertically results in a jet that is self-collimating. The effect of the self-collimation on the dynamics was not previously considered in *agnjet*. We show here that the effect is small as long as the initial cross-sectional radius of the jet is roughly equal to the launch height.

The cross-sectional radius of the jet, r , is assumed to follow

$$r = r_0 + (z - z_0) \gamma_0 \beta_0 / (\gamma_j \beta_j), \quad (27)$$

and conservation of number density of particles is

$$n = n_0 \left(\frac{\gamma_j \beta_j}{\gamma_0 \beta_0} \right)^{-1} \left(\frac{r}{r_0} \right)^{-2}. \quad (28)$$

For the quasi-isothermal case, i.e., what is currently used in *agnjet*, the internal energy profile is

$$U_j = \zeta n_0 m_p c^2 \left(\frac{\gamma_j \beta_j}{\gamma_0 \beta_0} \right)^{-\Gamma} \left(\frac{r}{r_0} \right)^{-2}. \quad (29)$$

($\zeta = 1$ in *agnjet*). With the cross-sectional radius assumed in Equation (27), the 1-D Euler equation becomes:

$$\left\{ \gamma_j \beta_j \frac{\Gamma + \xi}{\Gamma - 1} - \Gamma \gamma_j \beta_j - \frac{\Gamma}{\gamma_j \beta_j} + \frac{2(z - z_0) \gamma_0 \beta_0 / (\gamma_j \beta_j)}{r_0 \gamma_j \beta_j + \gamma_0 \beta_0 (z - z_0)} \right\} \times \frac{\partial \gamma_j \beta_j}{\partial z} = \frac{2\gamma_0 \beta_0}{r_0 \gamma_j \beta_j + \gamma_0 \beta_0 (z - z_0)}; \quad (30)$$

and as before,

$$\xi = \frac{1}{\zeta} \left(\frac{\gamma_j \beta_j}{\gamma_0 \beta_0} \right)^{\Gamma-1}; \quad \gamma_0 \beta_0 = \sqrt{\frac{\zeta\Gamma(\Gamma - 1)}{1 + 2\zeta\Gamma - \zeta\Gamma^2}}. \quad (31)$$

There is now another free parameter in the velocity profile: the initial aspect ratio of the jet: r_0/z_0 . We show the effects of this new parameter and compare our results to a quasi-isothermal conical jet in Figure 3.

To divvy up the total internal energy into an electron energy density and magnetic energy density, *agnjet* uses a free parameter k , defined as the ratio of the magnetic energy density

to the electron energy density. The dependence of the magnetic field on the height is

$$B = \sqrt{\frac{8\pi k U_j}{1+k}}. \quad (32)$$

U_j has a height dependence that is different if the jet is assumed to be isothermal, quasi-isothermal, or adiabatic. In the isothermal jet, $B \propto r^{-1}(\gamma_j \beta_j)^{-1/2}$, which is slightly slower than the expected dependence if there is flux conservation of a toroidal magnetic field ($\propto r^{-1}(\gamma_j \beta_j)^{-1}$). In the adiabatic or quasi-isothermal case, the magnetic field decreases faster than in an isothermal jet. The electron's characteristic Lorentz factor γ_e has the same distance and bulk Lorentz factor dependence as the temperature. $\gamma_{e,0}$ is a free parameter. The density profile of the electrons is determined by number conservation, but the initial number of electrons and positrons is fixed by requiring that $U_{j,0} = n_p m_p c^2$,

$$\frac{n_e}{n_p} = \frac{1}{1+k} \frac{m_p}{\gamma_{e,0} m_e}. \quad (33)$$

The above relationship will break down if k is too large, and it results in a non-physical, electrostatically charged jet with $n_e < n_p$. k must satisfy the following inequality

$$k+1 \lesssim 110 \left(\frac{T_{e,0}}{10^{11} \text{ K}} \right)^{-1} \quad (34)$$

If *agnjet* requires a k large enough to violate the above inequality to fit the spectrum of an object, the k is inconsistent with the model of *agnjet*. In this case, it likely means that the jet is Poynting dominated, i.e., $U_B > U_p$, a scenario which is not considered in *agnjet*. We note that versions of *agnjet* prior to 2014 did not use eq (33) to set the number of electrons and positrons, and instead simply set $n_e = n_p$. In the earlier version, *agnjet* was only self-consistent if $1+k$ was equal to the right hand side of eq (34). If we force $n_e = n_p$, as in the earlier version of *agnjet*, when $1+k < 110 [T_{e,0}/(10^{11} \text{ K})]^{-1}$, the difference from a self-consistent solution can be estimated by solving the Euler equation in eq (30) with a $\zeta = (1+k) [T_{e,0}/(10^{11} \text{ K})] / 110$. The differences are likely to be minor even if $\zeta \ll 1$ because the jet is not accelerated very much even when $\zeta = 1$. If in the previous version of *agnjet* a solution was found with $1+k \gg 110 [T_{e,0}/(10^{11} \text{ K})]^{-1}$, the jet is Poynting dominated, and its dynamics are not correctly calculated by *agnjet*.

We plot an example multiwavelength spectral-energy distribution using *agnjet* in Figure 4. In the figure it is clear that the quasi-isothermal, isothermal, and previous *agnjet* with minor errors all give roughly the same result: a nearly flat, self-absorbed synchrotron spectrum at frequencies below the thermal bump, and a Compton hump in the X-rays. In Figure 4, we assume the jet to be self-collimating when calculating the dependence of the internal energy of the jet with height, but we use the velocity profiles from Figure 1. Unlike the models with a constant or nearly-constant temperature throughout the jet, the adiabatic model shows a steep rise from the self-absorbed radio emission to the thermal synchrotron bump. We find that to have a flat radio spectra the jet must be kept at a nearly constant temperature, a similar conclusion as found by Blandford & Königl (1979) when fitting the radio cores of AGNs or as found by Mościbrodzka & Falcke (2013) when fitting the radio spectrum of Sgr A*, or as found by Pe'er & Casella (2009) when fitting the radio emission of X-ray binaries.

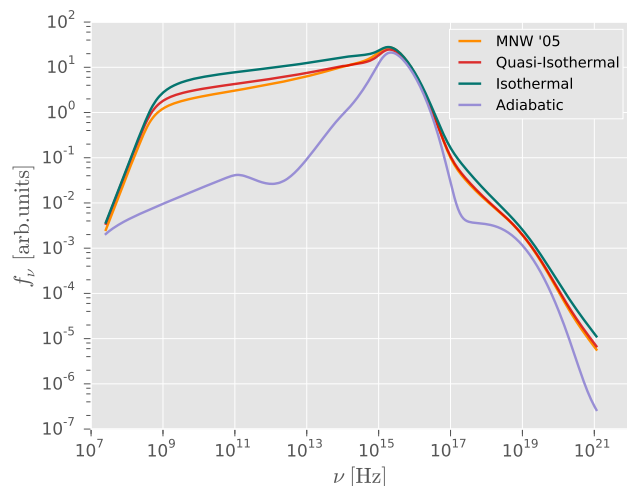


Fig. 4. This figure shows the different spectral energy distribution (SED) calculated for conical jets in *agnjet*. The colors correspond to the same Lorentz factor profiles in Figure 1. The models where the temperature is constant or nearly constant all show similar SED, while the adiabatic model has a steep rise below the thermal synchrotron bump.

5. Summary and Discussion

In this work, we have re-analyzed the hydrodynamical jets derived in Falcke (1996). When deriving the Lorentz factor profile, Falcke (1996) used the *maximal jet* model from Falcke & Biermann (1995), that contains an algebraic error. The *maximal jet* assumption has two main conclusions—the jet's power is dominated by its kinetic power, and the jet power must be less than the mass accretion rate of the disk onto the black hole times the bulk Lorentz factor of the jet. We argued in this letter that the second conclusion is likely true in general for astrophysical jets. Even in jets that extract their energy from the black-hole spin, the energy in the jet does not greatly exceed $\dot{M}_{BH} c^2$ because the amount of magnetic flux that can be carried to the black hole depends on the mass accretion rate. The maximal efficiency of jet production found in GRMHD simulations is $\lesssim 300\%$ (Tchekhovskoy et al. 2011; Nemmen & Tchekhovskoy 2015). Furthermore, while it is true that the jet's power need not be dominated by its kinetic power, we argued that this is a good approximation in a jet with a sufficiently small opening angle and a small terminal bulk Lorentz factor. X-ray binaries and low-luminosity AGN likely host such jets, so models based on these assumptions are well-founded for such objects. In addition, we corrected minor algebraic mistakes made in the derivation of the Lorentz factor profile from Falcke (1996). The effects of correcting these errors are to make the quasi-isothermal jet behave more similarly to a jet where the temperature is kept completely constant.

The Lorentz factor profile from Falcke (1996) was used in the *agnjet* model described in Markoff et al. (2005) & Maitra et al. (2009). *agnjet* has been used to fit the multiwavelength spectra of outflow dominated x-ray binaries and nearby low-luminosity active galactic nuclei. In *agnjet*, the jet is assumed to be self-collimating, but the collimation was not self-consistently applied to the jet's dynamics. We show that the effects of the self-collimation are negligible for quasi-isothermal jets as long as the aspect ratio of the jet at the launching point is of order unity. We examined the effects of the new Lorentz factor profile on the spectral energy distribution calculated by *agnjet*. We find there is very little difference between the

assumed quasi-isothermal jet and a completely isothermal jet, however, we find a large difference in the spectral energy distribution between an adiabatic jet and a jet where the temperature is kept roughly constant. We find that isothermal jets are required to match the flat radio spectra seen in hard/quiescent state XRB and low-luminosity AGN. We do not self-consistently account for how the jet is kept hot. If the jet is heated internally, the heating mechanism would change the Lorentz factor profile from the one calculated in this work. If the gas is shock heated, the shocks will change the jet's momentum, and if the jet is Poynting dominated, the dissipation of the magnetic field to heat the particles will change the magnetic pressure gradient.

Finally, we note that in addition to this work, there is an ongoing effort to derive a MHD-consistent jet model that will be capable of calculating the jet properties self-consistently, e.g. Polko et al. (2010, 2013, 2014), Ceccobello et al. *in prep.* Such models will be able to address many of the short-comings of the models described in this work.

Acknowledgements. PC would like to thank Heino Falcke, Peter Biermann, Sera Markoff, Pawan Kumar, Rodolfo Barniol Duran, and Thomas D. Russell for valuable discussions. PC acknowledges financial support from the WARP program of the Netherlands Organisation for Scientific Research (NWO). CC and RC acknowledge NWO/Nova. YC is supported by the European Union's Horizon 2020 research and innovation programme under the Marie Skłodowska-Curie Global Fellowship grant agreement No 703916.

References

- Blandford, R. D. & Königl, A. 1979, *ApJ*, 232, 34
 Blandford, R. D. & Payne, D. G. 1982, *MNRAS*, 199, 883
 Blandford, R. D. & Znajek, R. L. 1977, *MNRAS*, 179, 433
 Brinkerink, C. D., Falcke, H., Law, C. J., et al. 2015, *A&A*, 576, A41
 Connors, R. M. T., Markoff, S., Nowak, M. A., et al. 2017, *MNRAS*, 466, 4121
 Falcke, H. 1996, *ApJ*, 464, L67
 Falcke, H. & Biermann, P. L. 1995, *A&A*, 293
 Falcke, H., Markoff, S., & Bower, G. C. 2009, *A&A*, 496, 77
 Gallo, E., Fender, R. P., & Pooley, G. G. 2003, *MNRAS*, 344, 60
 Goldreich, P. & Julian, W. H. 1970, *ApJ*, 160, 971
 Granot, J., Komissarov, S. S., & Spitkovsky, A. 2011, *MNRAS*, 411, 1323
 Heinz, S. & Merloni, A. 2004, *MNRAS*, 355, L1
 Kalemci, E., Begelman, M. C., Maccarone, T. J., et al. 2016, *MNRAS*, 463, 615
 Komissarov, S. S. 1994, *MNRAS*, 269, 394
 Komissarov, S. S. 2011, *Mem. Soc. Astron. Italiana*, 82, 95
 Komissarov, S. S., Barkov, M. V., Vlahakis, N., & Königl, A. 2007, *MNRAS*, 380, 51
 Königl, A. 1980, *Physics of Fluids*, 23, 1083
 Kumar, P. & Zhang, B. 2015, *Phys. Rep.*, 561, 1
 Maitra, D., Markoff, S., Brocksopp, C., et al. 2009, *MNRAS*, 398, 1638
 Malzac, J. 2013, *MNRAS*, 429, L20
 Markoff, S., Nowak, M., Young, A., et al. 2008, *ApJ*, 681, 905
 Markoff, S., Nowak, M. A., Gallo, E., et al. 2015, *ApJ*, 812, L25
 Markoff, S., Nowak, M. A., & Wilms, J. 2005, *ApJ*, 635, 1203
 McKinney, J. C. 2006, *MNRAS*, 368, 1561
 Miller-Jones, J. C. A., Fender, R. P., & Nakar, E. 2006, *MNRAS*, 367, 1432
 Miller-Jones, J. C. A., Rupen, M. P., Fender, R. P., et al. 2007, *MNRAS*, 375, 1087
 Mościbrodzka, M. & Falcke, H. 2013, *A&A*, 559, L3
 Muñoz-Darias, T., Casares, J., Mata Sánchez, D., et al. 2016, *Nature*, 534, 75
 Muñoz-Darias, T., Casares, J., Mata Sánchez, D., et al. 2017, *MNRAS*, 465, L124
 Narayan, R., Igumenshchev, I. V., & Abramowicz, M. A. 2003, *PASJ*, 55, L69
 Neilsen, J. & Lee, J. C. 2009, *Nature*, 458, 481
 Nemmen, R. S. & Tchekhovskoy, A. 2015, *MNRAS*, 449, 316
 Pe'er, A. & Casella, P. 2009, *ApJ*, 699, 1919
 Plotkin, R. M., Gallo, E., Markoff, S., et al. 2015, *MNRAS*, 446, 4098
 Polko, P., Meier, D. L., & Markoff, S. 2010, *ApJ*, 723, 1343
 Polko, P., Meier, D. L., & Markoff, S. 2013, *MNRAS*, 428, 587
 Polko, P., Meier, D. L., & Markoff, S. 2014, *MNRAS*, 438, 959
 Pomraning, G. C. 1973, *The equations of radiation hydrodynamics*
 Tchekhovskoy, A., Narayan, R., & McKinney, J. C. 2011, *MNRAS*, 418, L79
 van Oers, P., Markoff, S., Rahoui, F., et al. 2010, *MNRAS*, 409, 763
 Vlahakis, N. & Königl, A. 2003, *ApJ*, 596, 1080
 Zdziarski, A. A. 2016, *A&A*, 586, A18